

PAPER • OPEN ACCESS

Development of high-effective superconducting single-photon detectors aimed for mid-IR spectrum range

To cite this article: P I Zolotov *et al* 2017 *J. Phys.: Conf. Ser.* **917** 062037

View the [article online](#) for updates and enhancements.

Development of high-effective superconducting single-photon detectors aimed for mid-IR spectrum range

P I Zolotov^{1,2}, A V Divochiy², Yu B Vakhtomin^{1,2}, P V Morozov², V A Seleznev^{1,2} and K V Smirnov^{1,2,3}

¹Moscow State Pedagogical University, Moscow 119435, Russia

²JSC «Superconducting Nanotechnology» (SCONTEL), Moscow 119021, Russia

³National Research University Higher School of Economics, Moscow 101000, Russia

E-mail: zolotov@scontel.ru

Abstract. We report on development of superconducting single-photon detectors (SSPD) with high intrinsic quantum efficiency in the wavelength range 1.31 – 3.3 μm . By optimization of the NbN film thickness and its compound, we managed to improve detection efficiency of the detectors in the range up to 3.3 μm . Optimized devices showed intrinsic quantum efficiencies as high as 10% at mid-IR range.

1. Introduction

Recent years have seen ultimate growth of interest in sphere of quantum communication and quantum computation systems. Such experiments usually require single-photon-counting solutions with ultimate timing and efficiency characteristics. Perfect example of such devices are SSPDs which took the leadership over other photon-counting technologies in near-IR spectrum range due to its excellent values of the timing resolution, counting rate and detection efficiency [1, 2, 3, 4]. Fiber-optic-based setups, which used in a wide range of experiments [5, 6], significantly reduce possible field of implementation of SSPDs, which are expected to have wide spectrum band up to mid-IR range. Due to the fact, that absorbance and quantum output (the number of emerged from absorbed photon quasiparticles) are the only restrictive parameters for SSPD's wideband operation, the optical cavity usually employed to increase poor absorbance of the structured film [7]. However, improvement of the intrinsic quantum efficiency of the device stays not a trivial task. As it has been shown [8, 9], decreasing the strip width below 50 nm results in extending of the sensitivity of SSPD at mid-IR range. Because decreasing the strip width usually leads to the appearance of constrictions of the nanowire and therefore of significant drop of its critical current density (J_c), it is important to develop a new technology of fabrication of the device, which will allow its ultimate spectrum capabilities and high quantum efficiency simultaneously.

This study involves optimization of the films deposition process. Aiming to increase the quantum output of the photons with energies in the range 0.9-0.4 eV (1.3-3.3 μm) we decided to reduce films' critical temperature (T_c) by means of decreasing its thickness and by small variation of its compound, which led to the growth of the intrinsic quantum efficiency of the devices. Our goal was to make first fast and sensitive single-photon-counting solution for spectrum range above 1.7 μm , which could significantly accelerate development of single- and multi-photon sources in this spectrum range, for example quantum dots and semiconductor lasers, required in a broad band of applications, such as free-space optical communication and photoemission microscopy [10, 11, 12].



2. Implementation methods

The single-photon detection efficiency (η) is defined as the ratio of the measured number of counts to the number of photons incident on the device active area. η can be written as the product of the device absorbance α to the nanowire intrinsic single-photon detection efficiency (η_{in}), i.e. the probability that absorbed photon triggers the output voltage pulse. Nowadays, problem of poor absorbance of ultra-thin structured films can be fixed using integrated cavity designed to concentrate electric field in the nanowires, which increases the absorption up to the values of 95% [13, 14, 15]. However, achievement of high detection efficiency is impossible in case, when $\eta_{in} < 1$. Being associated with the quantum output, intrinsic quantum efficiency is dependent on photon energy. Thus, increasing the wavelength of incident radiation should be compensated by increasing of the current density or decreasing of the nanowire cross-section. As it was mentioned earlier, decreasing the width of the stripe comes with technological difficulties, however, decreasing film thickness could be done without major drawbacks. It is known that reduction of the film thickness leads to reduction of its T_c . Owing to the proportional decreasing of Δ and T_c parameters, quantum output of the photon is increased in this case, which results in growth of intrinsic quantum efficiency of SSPD.

To optimize sheet resistance (R_s), T_c and Residual-Resistance Ratio (RRR) values we made a series of film deposition processes. Films for our study were deposited using reactive magnetron sputtering technique with AJA INTERNATIONAL Inc. Orion-8 setup, which allows background pressure of $6 \cdot 10^{-8}$ Torr. By changing N_2 to Ar ratio in gas mixture for each deposition process, we managed to obtain films with various values of the main parameters. Variation of RRR allowed us to obtain films with high values of R_s at close-to-transition temperatures and to optimize proximity of our detectors to saturation of intrinsic quantum efficiency at biasing currents (I_b) close to the critical value (I_c). The authors elsewhere will publish detailed research on relation between film parameters and SSPD performance soon. Exact values of T_c , R_s and RRR for selected film in given research were 9.4 K, 630 Ohm/ \square and 0.74 respectively. Fabrication of SSPD continued with formation of the meander pattern with Jeol GSM6380 scanning electron microscope self-altered to e-beam lithography setup with approx. 3.5 nm resolution. Meanders had 100 nm wide strips with filling factor of 0.5 and cover-area of $15 \times 15 \mu m^2$. Ti-Au metallization layer was deposited by e-beam evaporation and then formed to the contact metallization by means of *lift-off* process. Unwanted NbN areas were plasma-etched in SF_6 using Corial 200R. At final step wafer was scribed into separate chips.

3. Experimental results and discussion

In order to sort-out defective devices, we electrically and optically characterized them. Devices with close-to-calculated values of resistance we tested in liquid helium in order to determine its T_c and I_c which allowed us to choose detectors with maximal uniformity of the strip (which corresponds to maximal density of critical current J_c) and lack of overetched regions (maximal T_c). Figure 1 represents histograms of resistance, critical current and quantum efficiency distributions for devices within the same batch.

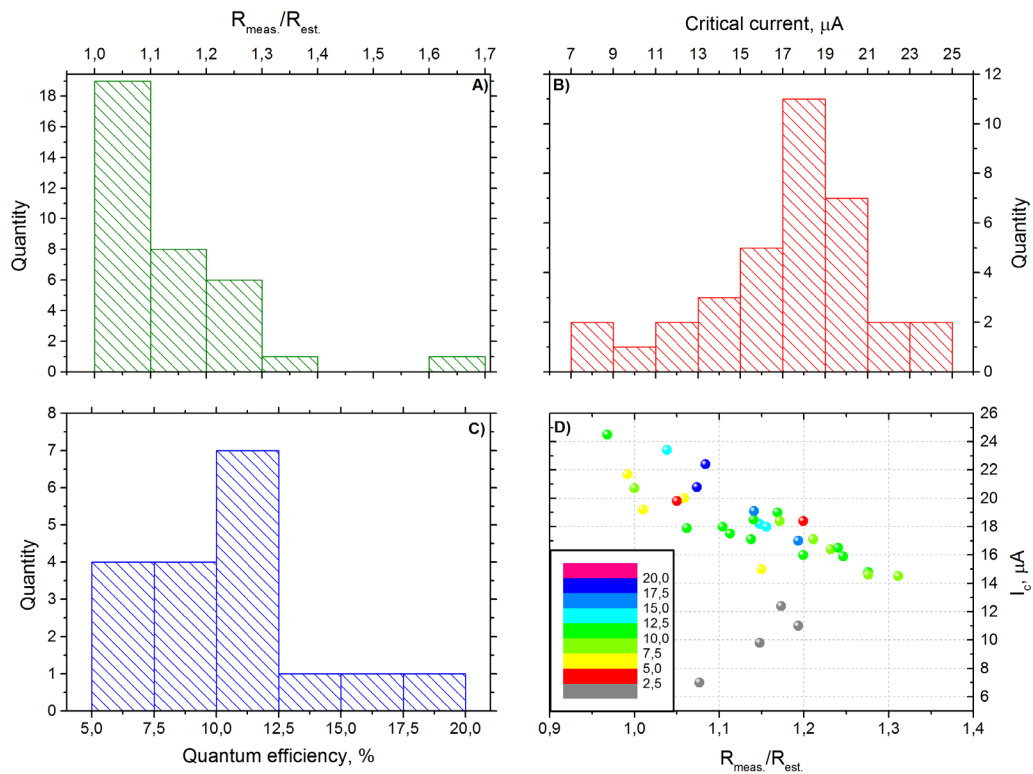


Figure 1. Statistics of the main parameters of fabricated devices within the same batch. A): Distribution of resistance of the devices measured at room temperature; B): histogram of critical currents of the devices at 4.2 K; C): distribution of quantum efficiencies (QE) of the devices at 1.55 μm at 4.2 K; D): critical current and resistance dependence of QE (marked in color).

Histogram **A)** of the resistance, i.e. relation of measured resistance of devices $R_{\text{meas.}}$ to thereof estimated values $R_{\text{est.}}$, distribution at room temperature show that 77% of SSPDs had $\sim 20\%$ deviation from calculated value of resistance. Histogram **B)** presents that majority of the devices from the batch (65%) had critical currents ranging from 15 to 21 μA . Taking into account film thickness (6 nm) and strip width, we can conclude that calculated J_c value of $2.5\text{-}3.3 \cdot 10^6 \text{ A/cm}^2$ fits to the highest standards for superconducting NbN films [16]. Quantum efficiency histogram at 1.55 μm **C)** has pronounced maximum which corresponds to 10-12.5% of measured quantum efficiency using standard technique [17] with free-space configuration which only allows initial characterization of the devices because of poor coupling of the detector with radiation, which estimated on the level of 30%. Presented histograms demonstrate that only 10% of the devices from the batch had low QE, with respect to the majority. Graph **D)** shows that for the greater number of devices from the batch J_c linearly drops with the growth of the nanowire resistance. For such detectors its QE corresponds to the maximal value from the histogram. This explains hypothesis of the presence of narrowed regions of the stripe for some devices with lower than optimal critical currents. Thus, it could be summarized that based on demonstrated histograms our SSPD batch had high from-chip-to-chip uniformity with almost 90% of the devices having similar parameters.

Among tested specimens, we selected those, which had close parameters. Each of these devices was placed in holder made of oxygen-free copper and fixed on cold plate of Gifford-McMahon (GM) cryocooler. As a light source we used grating monochromator with wavelength selectivity of 0.1 nm. Optical input of the cryostat with Si window allowed transmittance of radiation in selected wavelength range. Si window also acted as a high-effective filter for short-wave half-wavelength harmonics of

desired wavelength region, which usually presents on monochromator output. For measurements at wavelengths, starting from 2.2 μm as filter for half-wavelength harmonics we additionally used 3-mm thick Ge plate. To electrically bond SSPD with input/output channel, we used tpt HB12 wire bonder. Because our goal did not require any measurements of the detector input optical power, we did not create any precision coupling setup. Photon flux to the cryostat input was maintained at power level corresponding to 0.01-1 MHz counts of the device, minimizing saturation of the count rate and influence of dark counts on measured dependencies. In our experiment, we studied proximity of quantum efficiency of our devices to saturation level, i.e. proximity of intrinsic quantum efficiency to 1. Our study was performed in spectrum range 1.31-3.3 μm at temperature of 2.5 K. Results of the experiment are presented on Figure 2.

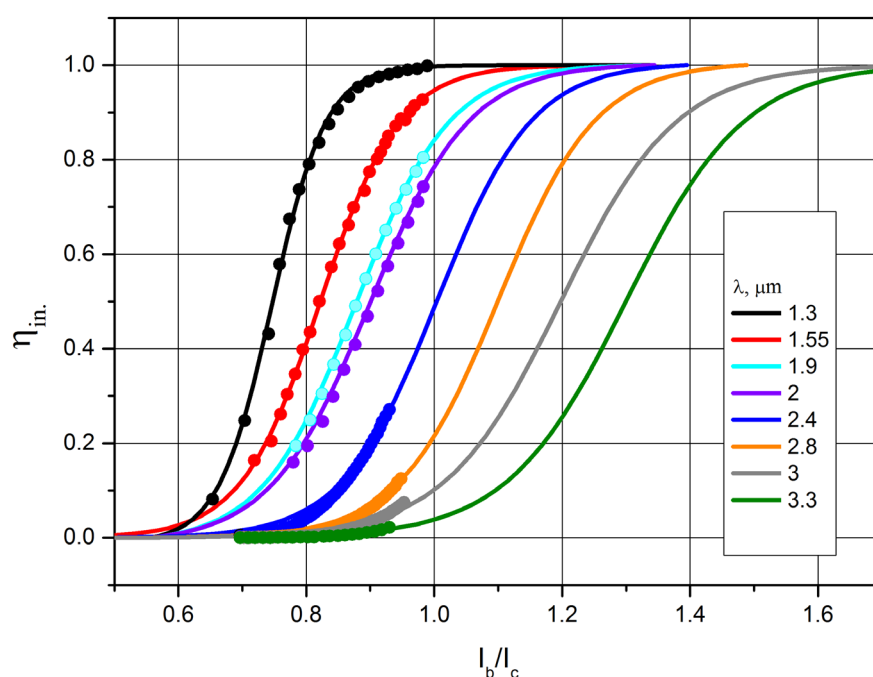


Figure 2. Results of bias current dependence of intrinsic quantum efficiency of SSPD at different wavelengths. Lines represent fitting curves and scatter – experimental results.

Presented graph show experimental curves fitted with sigmoidal function of obtained results allowing calculating exact level of η_{in} at selected wavelength. Values of intrinsic quantum efficiency varied from 1 to 0.04 corresponding to the spectrum range 1.31-3.3 μm , accordingly to the drop of photon energy. The shifting of the dependency to the region of higher currents with wavelength growth, as well as slope scaling, could be noticed. For example, curves corresponding to the wavelengths range of 2.8-3.3 μm matched values of internal efficiency ≤ 0.2 at I_c and reached values close to unity at currents as high as $1.5I_c$. Obtained results allow us to calculate possible detection efficiencies of the devices in cases of presence of optical resonator structure allowing to achieve high absorption at a given wavelength and in case of efficient coupling of the radiation to the sensitive area of the detector. Both of these goals have already been successfully implemented for visible \div near-IR range [13, 14, 18, 19], and therefore creating of the similar solutions for mid-IR region occur as a technical task.

Values of the fitting curves corresponding to the critical current of the detector at 2.5 K are plotted as a function of the wavelength on Figure 3. On the basis of our simulations, quantum efficiency of our detectors could be estimated as 40% and 10% at 2.5 μm and 3 μm respectively.

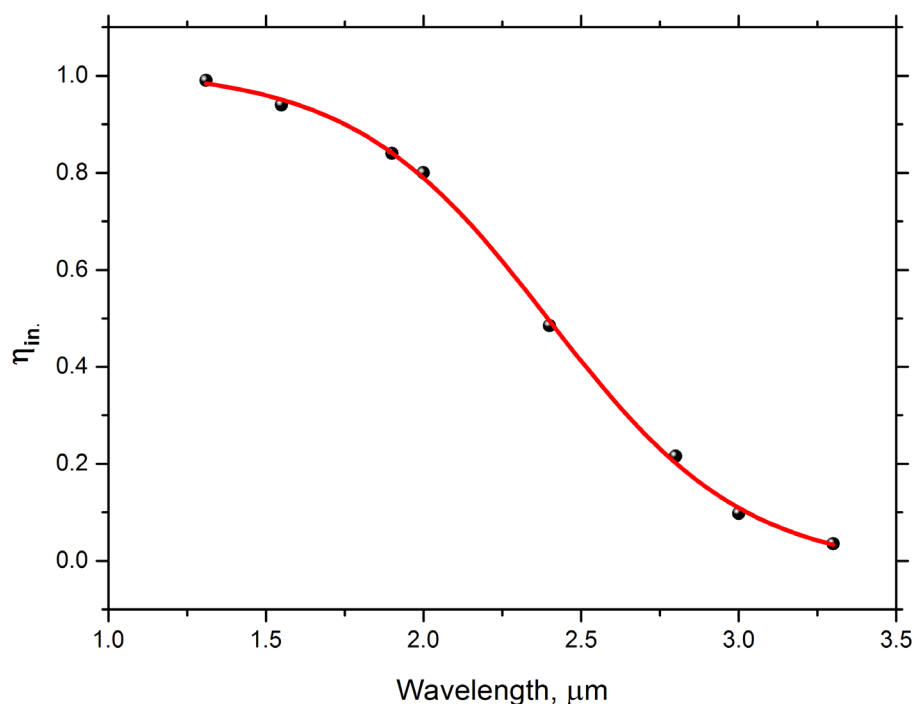


Figure 3. Spectral dependence of intrinsic quantum efficiency (dots) and fitting of the obtained results (line).

4. Conclusion

We have demonstrated capabilities of the SSPD fabricated from film with optimized parameters at mid-IR range. Obtained values of intrinsic quantum efficiency verify our improvements of the device qualities and enable the development of first fast and sensitive single-photon-counting systems for mid-IR spectrum range. By selection of different coupling method, this detector system could efficiently cover wavelength region from 1.3 to 3.3 μm .

References

- [1] Zadeh, I.E., Los, J.W., Gourgues, R., Steinmetz, V., Dobrovolskiy, S.M., Zwiller, V. and Dorenbos, S.N., 2016. Single-photon detectors combining near unity efficiency, ultra-high detection-rates, and ultra-high time resolution. arXiv preprint arXiv:1611.02726.
- [2] V. Shcheslavskiy, P. Morozov, A. Divochiy, Yu. Vakhtomin, K. Smirnov and W. Becker "Ultrafast time measurements by time-correlated single photon counting coupled with superconducting single photon detector" Rev. Sci. Instrum. 87, 053117 (2016).
- [3] Junjie Wu, Lixing You, Sijing Chen, Hao Li, Yuhao He, Chaolin Lv, Zhen Wang, and Xiaoming Xie, "Improving the timing jitter of a superconducting nanowire single-photon detection system," Appl. Opt. 56, 2195-2200 (2017)
- [4] K. Smirnov, Yu. Vachtomin, A. Divochiy, A. Antipov and G. Goltsman "Dependence of dark count rates in superconducting single photon detectors on the filtering effect of standard single mode optical fibers" 2015. Appl. Phys. Express 8, 022501.
- [5] N.R. Gemmell, A. McCarthy, B. Liu, M.G. Tanner, S.D. Dorenbos, V. Zwiller, M.S. Patterson, G.S. Buller, B.C. Wilson, and R.H. Hadfield, "Singlet oxygen luminescence detection with a fiber-coupled superconducting nanowire single-photon detector," Opt. Exp., vol.21, no.4, pp.5005–5013, 2013.
- [6] "Superconducting Devices in Quantum Optics," Eds. R.H. Hadfield and G. Johanson, Springer 2016.

- [7] Anant, V., Kerman, A.J., Dauler, E.A., Yang, J.K., Rosfjord, K.M. and Berggren, K.K., 2008. Optical properties of superconducting nanowire single-photon detectors. *Optics Express*, 16(14), pp.10750-10761.
- [8] Marsili, F., Najafi, F., Dauler, E., Bellei, F., Hu, X., Csete, M., ... & Berggren, K. K. (2011). Single-photon detectors based on ultranarrow superconducting nanowires. *Nano letters*, 11(5), 2048.
- [9] Marsili, F., Bellei, F., Najafi, F., Dane, A.E., Dauler, E.A., Molnar, R.J. and Berggren, K.K., 2012. Efficient single photon detection from 500 nm to 5 μm wavelength. *Nano letters*, 12(9), pp.4799-4804.
- [10] Vadim V. Vorobyov, Alexander Yu. Kazakov, Vladimir V. Soshenko, Alexander A. Korneev, Mikhail Y. Shalaginov, Stepan V. Bolshedvorskii, Vadim N. Sorokin, Alexander V. Divochiy, Yury B. Vakhtomin, Konstantin V. Smirnov, Boris M. Voronov, Vladimir M. Shalaev, Alexey V. Akimov, and Gregory N. Goltsman, "Superconducting detector for visible and near-infrared quantum emitters [Invited]," *Opt. Mater. Express* 7, 513-526 (2017)
- [11] Yamashita, T., Liu, D., Miki, S., Yamamoto, J., Haraguchi, T., Kinjo, M., Hiraoka, Y., Wang, Z. and Terai, H., 2014. Fluorescence correlation spectroscopy with visible-wavelength superconducting nanowire single-photon detector. *Optics express*, 22(23), pp.28783-28789.
- [12] Grein, M., Dauler, E., Kerman, A., Willis, M., Romkey, B., Robinson, B., Murphy, D. and Boroson, D., 2015. A superconducting photon-counting receiver for optical communication from the Moon. *SPIE Newsroom*, July.
- [13] F. Marsili, V.B. Verma, J.A. Stern, S. Harrington, A.E. Lita, T. Gerrits, I. Vayshenker, B. Baek, M.D. Shaw, R.P. Mirin, and S.W. Nam, "Detecting single infrared photons with 93% system efficiency," *Nat. Photon.* vol.7, no.3, pp.210–214, 2013.
- [14] V.B. Verma, B. Korzh, F. Bussieres, R.D. Horansky, S.D. Dyer, A.E. Lita, I. Vayshenker, F. Marsili, M.D. Shaw, H. Zbinden, R.P. Mirin, and S.W. Nam, "High-efficiency superconducting nanowire singlephoton detectors fabricated from MoSi thin-films," *Opt. Exp.*, vol.23, no.26, pp.33792–33801, 2015
- [15] Yamashita, T., Waki, K., Miki, S., Kirkwood, R.A., Hadfield, R.H. and Terai, H., 2016. Superconducting nanowire single-photon detectors with non-periodic dielectric multilayers. *Scientific reports*, 6.
- [16] Semenov, A., Günther, B., Böttger, U., Hübers, H.W., Bartolf, H., Engel, A., Schilling, A., Ilin, K., Siegel, M., Schneider, R. and Gerthsen, D., 2009. Optical and transport properties of ultrathin NbN films and nanostructures. *Physical Review B*, 80(5), p.054510.
- [17] Sidorova, M.V., Divochiy, A.V., Vakhtomin, Y.B. and Smirnov, K.V., 2015. Ultrafast superconducting single-photon detector with a reduced active area coupled to a tapered lensed single-mode fiber. *Journal of Nanophotonics*, 9(1), pp.093051-093051.
- [18] W. Slysz, M. Wegrzecki, J. Bar, M. Gorska, V. Zwiller, C. Latta, P. Bohi, I. Milostnaya, O. Minaeva, A. Antipov, O. Okunev, A. Korneev, K. Smirnov, B. Voronov, N. Kaurova, G. Gol'tsman, A. Pearlman, A. Cross, I. Komissarov, A. Verevkin, R. Sobolewski, "Fiber-coupled single-photon detectors based on NbN superconducting nanostructures for practical quantum cryptography and photon-correlation studies", *Appl. Phys. Lett.* 88, 261113 (2006)
- [19] Korneev, A., Korneeva, Y., Manova, N., Larionov, P., Divochiy, A., Semenov, A., Chulkova, G., Vachtomin, Y., Smirnov, K. and Goltsman, G., 2013. Recent nanowire superconducting single-photon detector optimization for practical applications. *Ieee Transactions on Applied Superconductivity*, 23(3), pp.2201204-2201204.